The effect of fibrillar matrix architecture on tumor cell invasion of physically challenging environments

A. Guzman, M.J. Ziperstein, L.J. Kaufman*

Department of Chemistry, Columbia University, New York, NY 10027

*corresponding author: kaufman@chem.columbia.edu

Supplementary Information

Matrix	***Storage modulus G' (Pa)***	***Pore size (μm)***
1.0 mg/ml AS 22˚C	5 ± 1	14.8 ± 2.2
1.0 mg/ml AS 37˚C	3.0 ± 0.3	6.7 ± 1.7
4.0 mg/ml AS 22˚C	351 ± 31	5.6 ± 0.8
4.0 mg/ml AS 37˚C	75 ± 9	1.7 ± 0.2
1.0 mg/ml PT	9 ± 2	7.9 ± 1.7
4.0 mg/ml PT	278 ± 9	3.5 ± 1.9
1.0 mg/ml BME	0.13 ± 0.05	N/A
3.0 mg/ml BME	0.8 ± 0.3	N/A
4.5 mg/ml BME	3 ± 1	0.11 ± 0.07 [1]
1.0 mg/ml PT+1.0 mg/ml BME	12 ± 1	N/A
1.0 mg/ml PT+3.0 mg/ml BME	22 ± 3	N/A

Supplementary Table 1. Matrix type, storage modulus G', and calculated pore size. For details about rheology and pore size analysis, see Materials and Methods. For matrices containing BME, confocal reflectance microscopy can not reveal pore size and therefore pore size is not available (N/A) for these gels except when reported elsewhere [1].

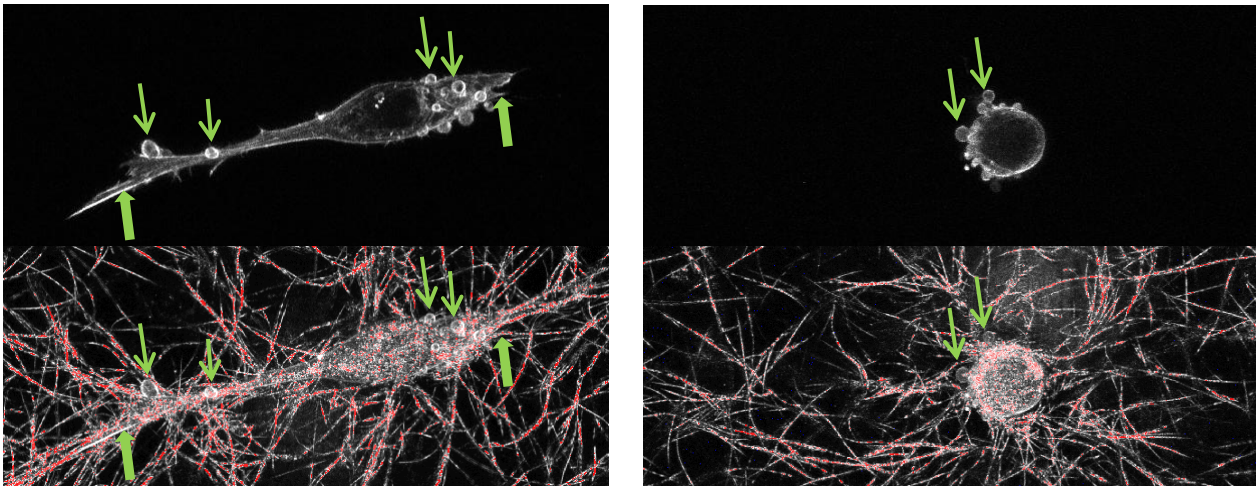

Supplementary Figure 1. Cell morphology and protrusions in 3D matrices. Cells embedded in 3D matrices were fixed, and the actin cytoskeleton was stained with fluorescently labeled phalloidin. Z-stacks of cells and surrounding collagen were taken by recording slices every 2.5µm with confocal fluorescence and reflectance microscopy, respectively. Two representative cells with different morphology and protrusions are shown. The upper panel shows the maximum projection of the fluorescence image only while the lower panel shows the overlaid fluorescence and reflectance maximum projections. The cell at left is polarized and bears both filopodia (block arrows) and blebs (line arrows); this cell is also shown in Fig. 5. The cell at right is non-polarized and displays only blebs.

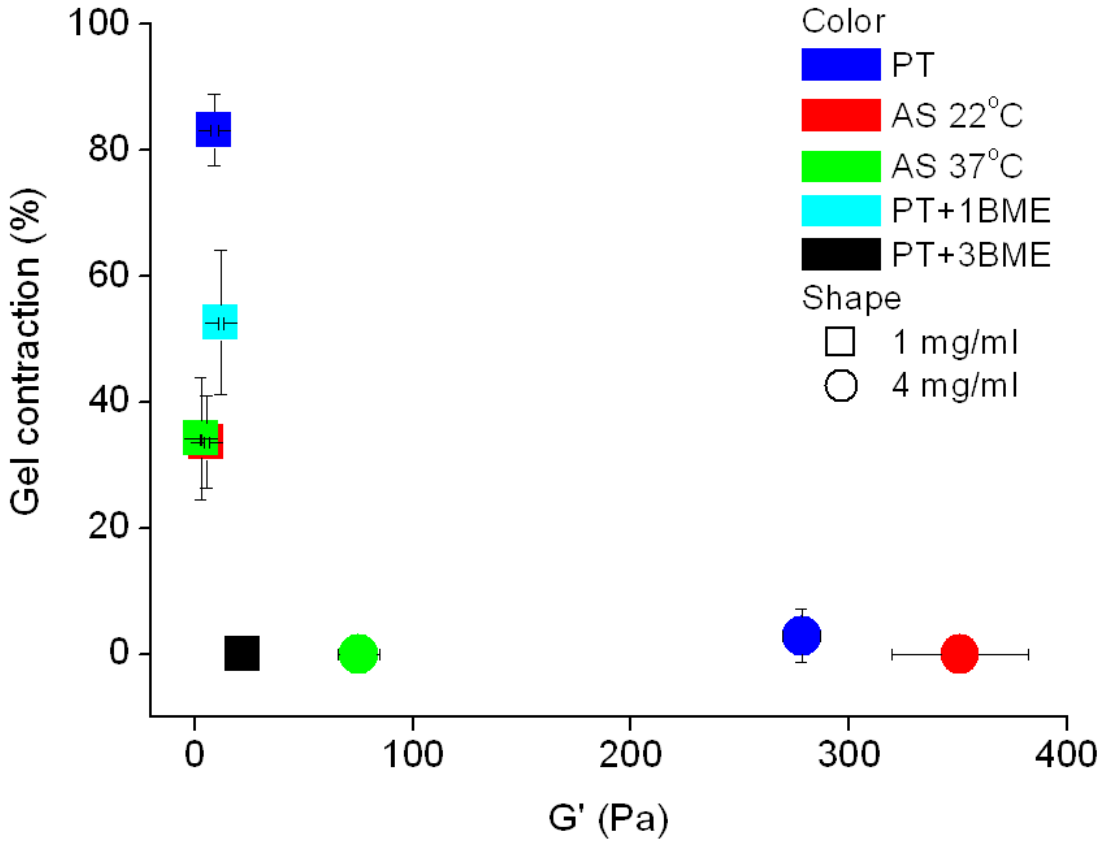

Supplementary Figure 2. Analysis of correlation between the degree of matrix contraction by dispersed cells and the viscoelastic properties of the matrix as reflected by storage modulus, G'. Efficient gel contraction was observed exclusively for fibrillar matrices with low storage moduli.

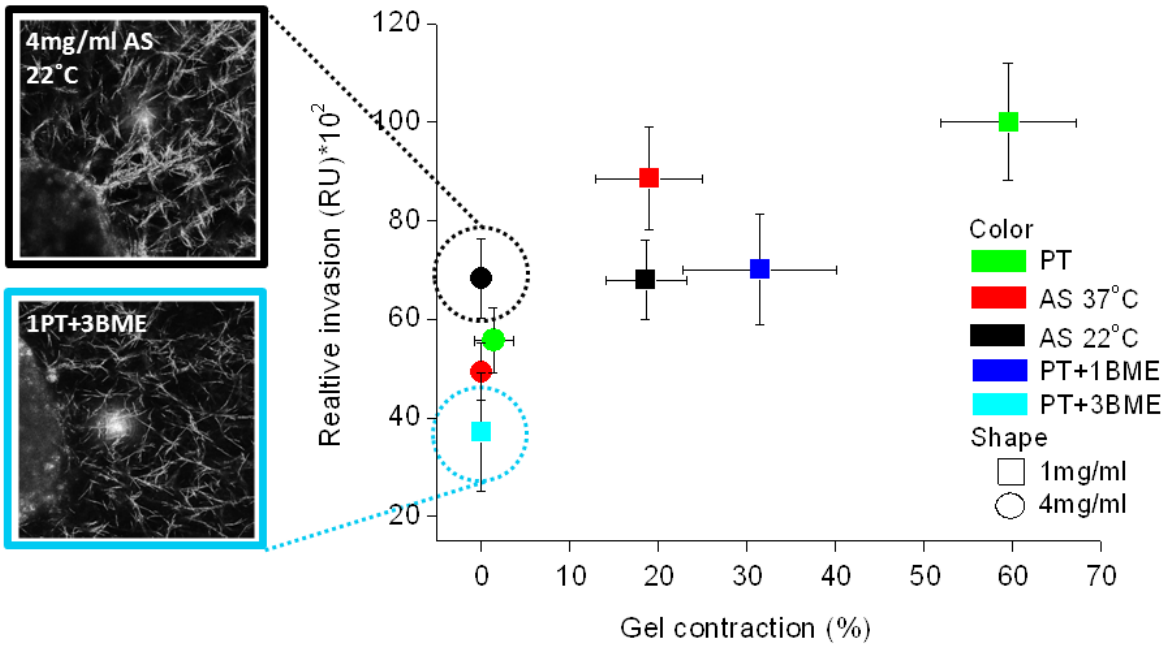

Supplementary Figure 3. Analysis of correlation between spheroid invasion and degree of gel contraction by dispersed cells in various types of matrices. Both responses were measured at t = 24 h. Mean values ± SD are depicted. While gels that were well contracted also supported significant invasion, some gels that could not be contracted also supported at least moderate invasion. The insets show CRM images of spheroids in two different 3D matrices at t = 2 h after implantation. While neither of the depicted matrices (4 mg/ml AS collagen gelled at 22˚C and 1 mg/ml PT collagen + 1 mg/ml BME) was contracted by individual cells, the collagen matrix was efficiently reorganized by spheroids, while the composite matrix was not. The degree of matrix reorganization – but not degree of matrix contraction – correlated with the invasive efficiency of spheroids in the matrices. Matrices that were more readily reorganized were also more readily invaded.

Reference

[1] Abrams GA, Goodman SL, Nealey PF, Franco M, Murphy CJ. Nanoscale topography of the basement membrane underlying the corneal epithelium of the rhesus macaque. Cell Tissue Res 2000;299:39-46.